1874-8368/19 *Send Orders for Reprints to reprints@benthamscience.net*

164

The Open Construction and Building Technology Journal

Content list available at: https://openconstructionandbuildingtechnologyjournal.com

RESEARCH ARTICLE

The Behavior of Concrete-Filled Single and Double-Skin uPVC Tubular Columns Under Axial Compression Loads

Abraham M. Woldemariam[1,*], Walter O. Oyawa[2] and Timothy Nyomboi[3]

[1]*Civil Engineering Department, PAUSTI, Jomo Kenyatta University of Agriculture and Technology, 62000 JKUAT, 00200 Nairobi, Kenya*
[2]*Civil, Const. and Environmental Engineering Department, Jomo Kenyatta University of Agriculture and Technology (JKUAT), PAUSTI and CUE, 62000 JKUAT; 00200 Nairobi, Kenya*
[3]*Department of Civil and Structural Engineering, PAUIST and Kenya Urban Roads Authority, 62000 JKUAT, 00200 Nairobi, Kenya*

Abstract:

Background:

There is an increased demand for high-performance materials in the construction industry due to high cost, difficulty of sourcing and shortcomings of the existing construction materials. Some of the deficiencies are corrosion of steel, brittle failure and rapid deterioration of reinforced concrete structures in a harsh environment. Nowadays, there is also a shift from one material to another due to the difficulty of sourcing *i.e.* timber electric poles to concrete poles due to the difficulty of sourcing. These situations have triggered the interest to develop an alternative structural system.

Objective:

This paper presents the behavior of unconfined concrete, Concrete-Filled Single Skin uPVC Tubular (CFSUT) and concrete-filled double skin uPVC tubular (CFDUT) members under axial compression loads.

Method:

The unconfined concrete cylinders, CFSUT and CFDUT specimens were prepared from a concrete class of C25 and tested using a UTM machine at a rate of 0.2MPa/s. The parameters considered included thickness to diameter ratio (2t/D), aspect ratio (h/D) and hollow ratio (d/D). Also, a model was developed to predict the peak strength of CFSUT and CFDUT specimens.

Results:

The result shows that both CFSUT and CFDUT specimens exhibited improved strength, ductility, and energy absorption capacity. For CFSUT and CFSUT specimens, the strength, ductility, and energy absorption capacity increased by more than 1.32, 3.75 and 14.75 times compared to the unconfined concrete specimens, respectively. It is found that the strength decreased as the h/D and d/D ratios increased. The result also shows that the strain of CFSUT and CFDUT at the peak strength increased by more than 3.16 times compared to the unconfined concrete specimens. The proposed model accurately predicted the peak strength with AAE of 2.13%.

Conclusion:

The uPVC confinement provided a remarkable improvement on the strength, ductility and energy absorption of concrete. Therefore, uPVC tubes can be used as a confining material for bridge piers, piles, electric poles, and building columns to increase strength, ductility and energy absorption of concrete structures.

Keywords: Concrete-filled uPVC tube, Double skin, Ductility, Energy absorption, Strength, Stress-strain.

Article History	Received: May 05, 2019	Revised: July 23, 2019	Accepted: July 26, 2019

1. INTRODUCTION

Composite materials are being widely used in the construction industry due to their good structural performance and economic advantages. Extensive studies have been conducted on the Concrete-Filled Steel Tube Columns (CFST) for the last six decades. Several advanced models were developed to predict the bearing capacity of the (CFST) columns [1]. In the past few years, studies on the use of uPVC tube as confinement and stay in place formwork for building columns, bridge piers, poles, highway head signs and piles have demonstrated the improved structural performance. Concrete-filled uPVC column com-bines the individual peak

* Address correspondence to this author at the Department of Civil Engineering Department, PAUSTI, Jomo Kenyatta University of Agriculture and Technology, 62000 JKUAT, 00200 Nairobi, Kenya; E-mail: abrish27@yahoo.com

performance of the uPVC tube (tensile strength and ductility) and concrete (compression). A number of experimental studies on uPVC confined concrete columns have been carried out [2 - 13]. uPVC lateral confinement increased the strength and ductility of concrete [2 - 9]. Woldemariam *et al.* [2] investigated the structural performance of uPVC confined concrete equivalent cylinder under axial compression loads. The result shows that the uPVC confinement increased the strength, ductility, and energy absorption in between 1.28-2.35, 1.84-15.3, and 11-243 times to un-confined levels, respectively. Similar studies had reported that the axial strength concrete columns had improved when the uPVC tube was used as a confining material. The strength of confined concrete was increased by 1.18 to 3.65 [4]; 11-17% [14]; 1.324 to 2.345 [15] and 1.352 to 2.100 [16] times to unconfined column. Also, the uPVC confinement contributed much to the ductility and energy absorption of the concrete. The ductility of confined concrete increased by 2.094 to 5.540 [15], 40% [7], 147.3% [11],1.30 to 2.65 [16] times to unconfined column.

In recent years, there is a development on another type of concrete-filled tubular columns, the double skin concrete-filled tubular column. The concrete is filled in between the two tubes (steel or FRP) to form a tubular column. Compared to the single skin concrete-filled tubular column, the double skin concrete-filled tubular column is light, more ductile and has high bending stiffness and better resistance to cyclic loading [17]. There are situations where the tubular section is preferred over solid sections. The hollow allows installing cables very simply in it, which gives a eustatic value. Nowadays, there is a shift from timber electric poles to concrete due to the difficulty of sourcing. The double skin concrete-filled tubular columns are very viable to use for bridge piers, highway head signs, electric and telecom utility poles. The high bending stiffens of double skin tubular section gives the advantage for a slender structural system such as electric poles. So far, studies conducted on the concrete-filled double-skin uPVC tube (CFDSUT) are limited. Many studies have been conducted on concrete-filled double skin steel tube (CFDST) [18 - 21], concrete-filled double skin stainless steel tube (CFDSST) [17, 22], double skin FRP-Concrete-Steel tubular columns and double skin concrete-filled FRP tubes. The studies have shown that the double-skin concrete-filled tubes are economical, quicker to construct and the hollow simplifies electrical wiring.

The purpose of this study is to investigate the structural performance of single and double skin concrete-filled uPVC columns subjected to axial compression loads. The columns with different hollow ratio were prepared and tested under axial compression load. A model was developed to predict the peak strength of CFSUT and CFDUT columns. In addition, the strength, ductility, energy absorption capacity, stress-strain behavior, and failure modes are reported.

2. EXPERIMENT PROGRAM

2.1. Materials

The Material characterization was completely described in the previous author's work [2], but it is briefly discussed here for clarification purpose. Ordinary Portland Cement (OPC) power plus 42.5N manufactured by Bamburi cement Ltd, Kenya conforming to the European Norm EN 197-1:2011 [23] and locally available natural sand from Masinga river (Kenya) and crushed stone obtained from Mlolongo (Kenya) were used throughout the experiment to prepare the concrete mix. The fine and coarse aggregate material characterization was done according to BS standard and the results are presented in Table **1**. The sampling was done according to BS EN 932-1, 1997 [24]. Both the fine and coarse aggregate were graded through sieving and curve plotting according to BS EN 12620: 2013; BS EN 933-1:2012 [25] and BS EN 933-2, 1996 [26]. Un-plasticized polyvinyl chloride (uPVC) pipes produced by Elson plastics ltd. was used for this research. The tensile property of uPVC tube was obtained through a tensile test of dogbone coupon specimens as shown in Fig. (**1**). The test was done by applying a constant rate of 5mm/min according to ASTM D638 [27] and the results are presented in Table **2**.

2.2. Concrete Mix Design and Fresh Properties of Concrete

The concrete mix design and the fresh properties of concrete were completely described in the previous authors' work [2]. The mix designs were prepared based on BS EN 206: 20134 [30] and BS EN 8500-1/2:2012 [31], and are summarized in Table **3**. Sampling, slump, density, and compaction factor tests were conducted in accordance with the procedures specified in BS EN 12350-1: 2009 [32], EN 12350-2: 2009 [33], BS EN 12350-6: 2009 [34], and BS 1881-103: 1993 [35] respectively. The results on the concrete mix and fresh properties of concrete are summarized in Tables **3** and **4**.

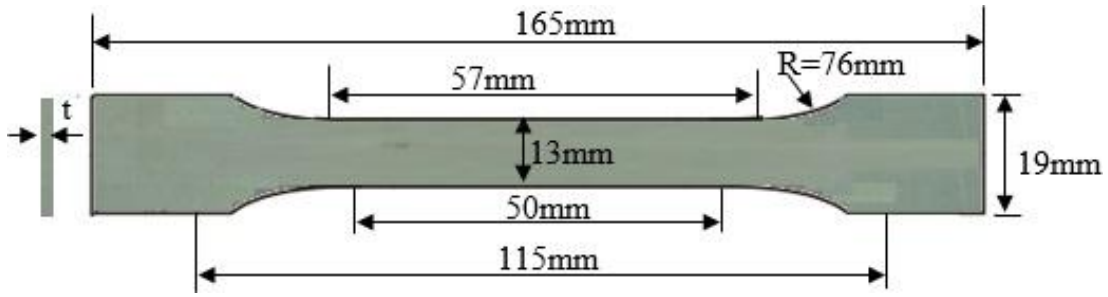

Fig. (1). Dog-bone Coupon specimens prepared from the uPVC tube (based on ASTM D638) [2].

Table 1. Aggregate Properties [2].

Test Type	Specific Gravity	Bulk Density	Water Absorption	Moisture Content	Fineness Modulus
Fine Aggregate	2.62	1479.96 kg/m^3	2.42%	0.28%	3.65
Coarse Aggregate	2.7	1420 kg/m^3	1.34%	1.42%	
Standard	BS EN 1097-6: 2013 [28]	BS EN 1097-6: 2013 [28]	BS EN 1097-6: 2013 [28]	BS EN 1097-5 2008 [29]	BS EN 1097-5 2008 [29]

Table 2. Average values of the tensile strength test for uPVC tube [2].

Parameter	Ultimate Tensile Strength (MPa)	Young's Modulus (GPa)	Poisson Ratio
Parallel to the Extrusion	49.74	3.58	0.342
Perpendicular to the Extrusion	50.10	3.61	0.339
Variance (%)	0.72	0.84	0.880

Table 3. Concrete mix-design [2].

Constituent Materials	Cement	Fine Aggregate	Coarse Aggregate	Total Water
Units	Kg/m^3	Kg/m^3	Kg/m^3	Kg/m^3
C25	360	602	1247	222

Table 4. Fresh properties of concrete mixes [2].

Fresh Property	Slump	Fresh Density	Compaction Factor
Units	mm	(kg/m^3)	-
C25	60	2433	0.935

2.3. Specimens Preparation

2.3.1. Single Skin Concrete-Filled uPVC Tubes

A total of 24 unconfined(plain) and Concrete-Filled Single Skin uPVC Tubular (CFSUT) specimens with different values of aspect ratio (h/D = 2,4 and 6), thickness to diameter ratio, and a concrete compressive strength of 25MPa was cast and tested to investigate the performance under axial compression loads as shown in Table **5**, Fig. (**2**) and Fig. (**5**). The uPVC tube was prepared by cutting a uPVC tube having a diameter of D=110 and 140mm and by varying the height to diameter ratio (h/D=2, 4 and 6) as shown in Fig. (**2a**). Unconfined concrete cylinders (ASTM C39-12 and C496-11) and uPVC confined concrete columns were cast by filling the wet concrete mix in three layers and compacting till no bubbles are seen on the surface (BS EN 12390-2:2009). After 24 hours the specimens were labeled based on concrete strength class (C3=C25), uPVC diameter (P2=90mm, P3=110mm and P4=140mm) and height to diameter ratio (H1=(h/D=2), H2=(h/D=4), H3=(h/D=6), and H4=(h/D=8); for example, C3P3H3 means a confined concrete cylinder having a concrete strength of C25, uPVC diameter of 110mm and aspect ratio of six (h/D=6).

Table 5. Specimen specification of single skin concrete-filled uPVC tube.

Label	Concrete Class	Diameter (mm)	Thickness of uPVC Tube (mm)	Height of the Specimens (mm)	Number of Specimens
C3	C25	100	-	200	3
C3	C25	110	-	220	3
C3P3H1	C25	110	3	220	3
C3P4H1	C25	140	3	280	3
C3P3H2	C25	110	3	440	3
C3P4H2	C25	140	3	560	3
C3P3H3	C25	110	3	660	3
C3P4H3	C25	140	3	840	3

2.3.2. Double Skin Concrete-Filled uPVC Tube

A total of 21 concrete-filled double skin uPVC tubular columns with C25, height to diameter ratio of (h/D =2, 4 and 6) and thickness of (D-d) = 53, 71 and 83mm were cast and tested as shown in Table **6**, Figs. (**3**, **4** and **5**). The columns were labeled based on the concrete strength class (C3=C25), thickness (D1= 53, D2=71 and D3=83) and aspect ratio of h/D =2, 4 and 6; For example, C3D1H2 means double skin with concrete class of C25, thickness (D-d) of 53mm and aspect ratio(h/D) of four.

Fig. (2). (a) Before concrete pouring, **(b)** Single skin.

2.4. Instrumentation, Test Setup and Loading Program

The instrumentation, test setup and loading program were completely described in the previous author's work [2], but are briefly discussed here for clarification purpose. After casting the specimens in water for 28 days, they were brought out from the water and the two sides of the specimens were smoothened using a concrete cutting machine to avoid a local buckling of the uPVC tube at the edge, and allowed to dry prior to testing as shown in Fig. (**2b**) and Fig. (**4b**). The test was performed using Compression Machine, which has a capacity of 2000kN and a testing frame with hydraulic loading jack connected to it as shown in Fig. (**5**). In addition, a load cell, transducers and strain gages connected to TDS-630 Datalogger were used to capture the measurements. First, the two strain gauges were placed on the surface of the specimen to measure the axial and radial strains. Then, the specimen was placed in between the two flattens of the compression testing machine, and also in between the upper and lower beam of the testing frame. Two LVDTs (Linear Variable Differential Transducers) were placed vertically, pointing to the moving plate of the machine to measure the axial deformation. After carefully placing the specimen in the testing machine, the strain gauges, load cells, and LVDTs were connected to TDS-630 data logger. The load was applied to the specimen at the rate of 0.2MPa/s till failure. The data was recorded both from the compression machine (Load-time data, Max. Load & Max. Strength) and TDS-630 Datalogger (time, Load, axial strain, radial strain, & displacement).

Table 6. Specimen specification of double skin concrete-filled uPVC tube.

Label	Concrete Class	D (mm)	d (mm)	Height, h (mm)	Number of Specimens
C3D1H1	C25	110	57	220	3
C3D2H1	C25	140	69	280	3
C3D3H1	C25	140	57	280	3
C3D1H2	C25	110	57	440	3
C3D3H2	C25	140	57	560	3
C3D1H3	C25	110	57	660	3
C3D3H3	C25	140	57	840	3

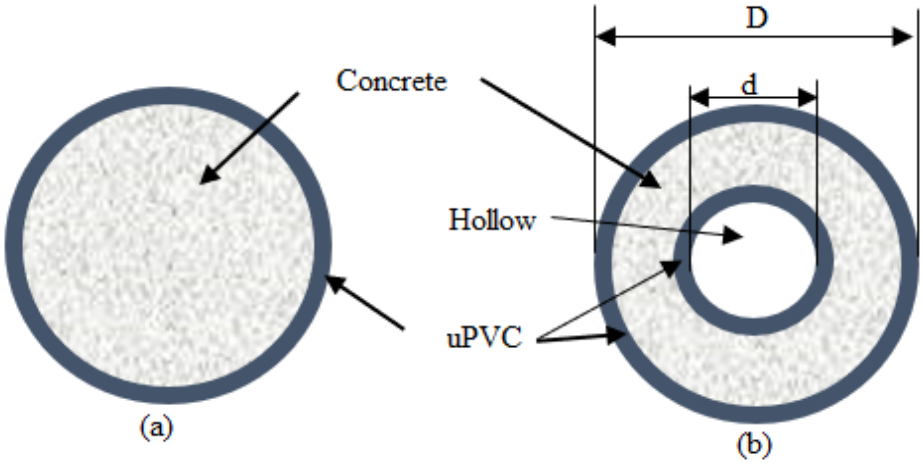

Fig. (3). (a) Single Layer **(b)** Double Layer (double skin).

Fig. (4). (a) Before concrete pouring, **(b)** Double skin.

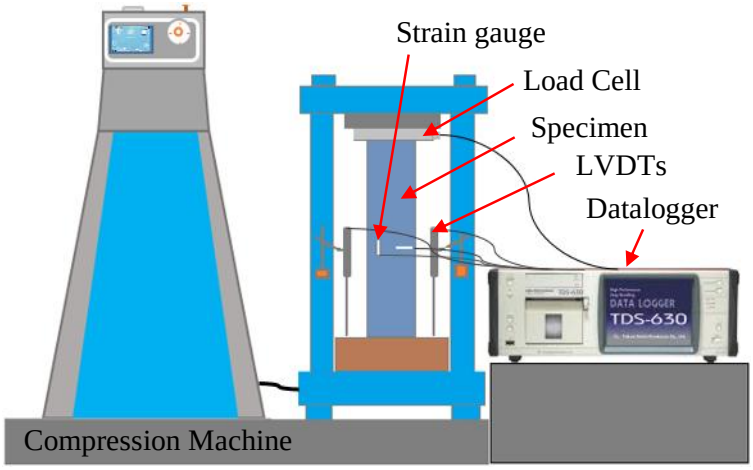

Fig. (5). Test set-up.

3. RESULTS AND DISCUSSIONS

3.1. Failure Modes

The failure modes of single and double skin concrete filled uPVC tube specimens are shown in Figs. (**6**, **7** and **8**). In contrast to the un-confined ones , all the confined (single and double skin) specimens showed a ductile failure. The Concrete-Filled Single Skin uPVC Tubular (CFSUT) specimens experienced drum, shear and buckling type failure. Different types of failure progression were observed in Concrete-Filled Double Skin uPVC Tubular (CFDUT) specimens, which are outward expansion making a drum type failure with local buckling of internal uPVC tube. Fig. (**6a**) shows the drum and shear-type failure modes of single skin concrete filled uPVC tube specimens. Drum type failure mode is the most prevalent type of failure observed during the experiment. The drum type failure mode is due to the type 2 and 3 failure modes (ASTM C39/C39M − 15a) of the core concrete. The shear-type failure mode was a observed event. The diagonal cracks of the concrete due to type 4 failure (ASTM C39/C39M − 15a) created the shear-type failure. Further loading the specimen pushed the two halves in the opposite direction on the inclined plane, creating a bump like structure. Fig. (**7**) shows the failure mode of double skin concrete filled uPVC tube specimens. The specimen expanded outside similar to the single skin creating drum-type failure. The internal tube has undergone local buckling (Fig. **7**). Buckling type failure mode was observed for higher aspect ratios for both single and double skin concrete filled uPVC tube specimens (Fig. **8**).

3.2. Strength and Strain Enhancement Ratio

Figs. (**9** and **10**) show the strength and strain enhancement ratio of unconfined concrete and single and double skin concrete-filled uPVC tube specimens. For both single and double skin specimens, the strength increased by more than 30% compared to the unconfined specimens. Similar researches that were done on single skin concrete-filled uPVC tube equivalent cylinders by Woldemariam *et al.* [2] showed that the strength enhancement ratio ranged was between 1.28 and 2.35 for different concrete strength and pipe size. Fig. (**10a**) shows the strain enhancement ratio of single skin and double skin concrete filled uPVC tube specimens at the peak load. For single and double skin specimens, the strain at peak load increased by more than 3 times compared to the unconfined specimen. Fig. (**10b**) shows the strain enhancement ratio of single and double skin at the failure load. It was observed that the strain at failure load increased by more than 9 times compared to the unconfined specimens.

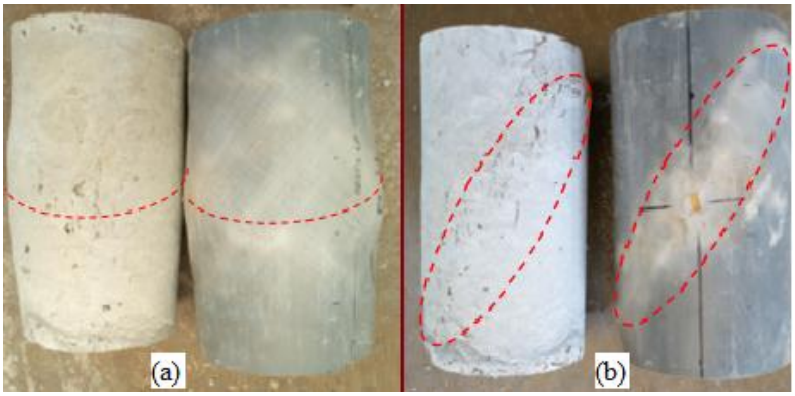

Fig. (6). Failure modes of single skin concrete filled uPVC tube specimens: **(a)** drum type, **(b)** shear.

Fig. (7). Failure modes of double skin concrete filled uPVC tube specimens (outward expansion and inner tube local buckling.

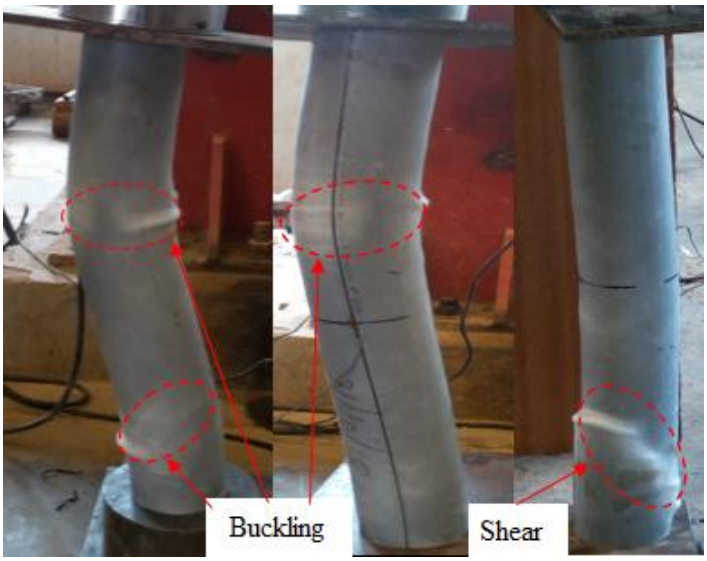

Fig. (8). Failure modes of single and double skin concrete filled uPVC tube specimens for higher aspect ratios.

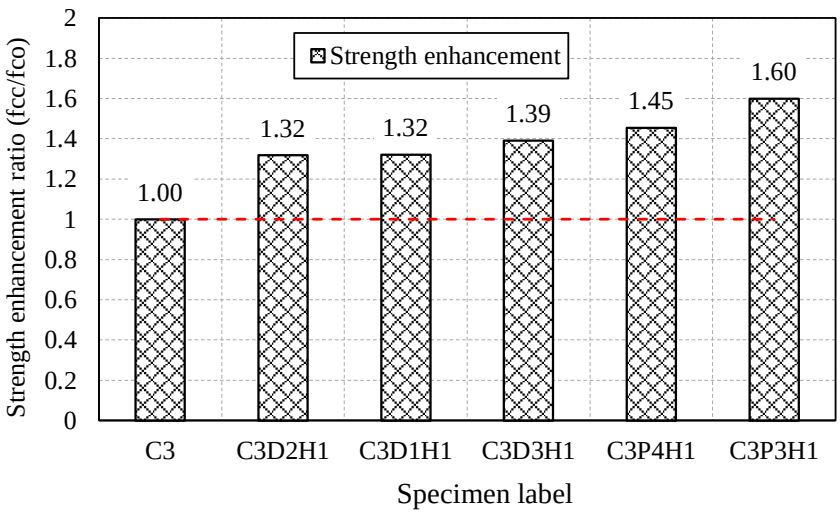

Fig. (9). Strength enhancement ratio (f_{cc}/f_{co}) .

3.3. Effect of Hollow Size

The recorded axial strength of concrete filled double skin uPVC tubular (CFDUT) specimens is presented in Table **7**, Figs. (**11** and **12**). The axial strength of (CFDUT) was obtained by testing the specimen under axial compression and compared with concrete filled single skin uPVC tubular (CFSUT) specimens. Figs. (**11** and **12**) show the relationship between the strength of single and double skin concrete-filled uPVC tube. For single skin, two types of uPVC tube size with a thickness of 3mm and a diameter of 110 and 140mm were used to prepare the specimens. The strength of (CFSUT) specimens were 26.99 and 24.57MPa. The strength decreased as the 2t/D ratio increased. The double skin specimen (CFDUT) was prepared from two uPVC tubes of the same height and different diameter where concrete is sandwiched in between the two tubes, as shown in Fig. (**3b**). To study the effect of hollow ratios on the axial strength, two different diameters of outer tubes (110 and 140mm) and inner (63 and 75mm) were used to prepare the specimens. The strength of the specimens decreased as the hollow ratio (d/D) increased.

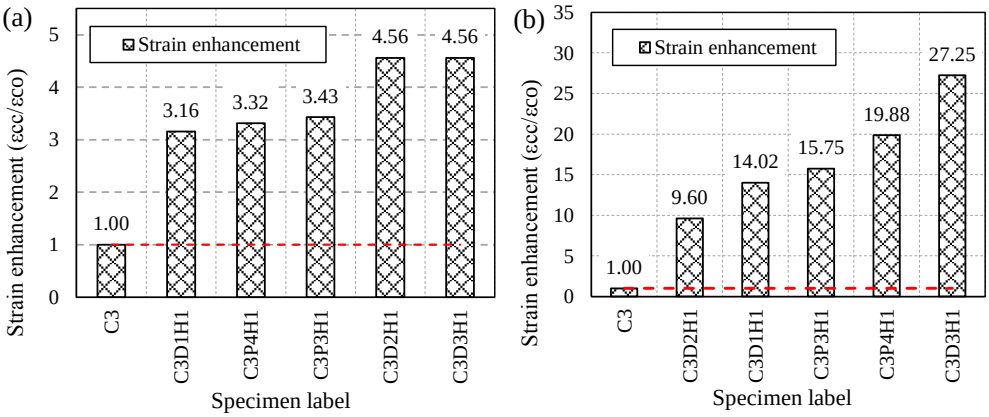

Fig. (10). Strain enhancement ratio at **(a)** peak strength $(\varepsilon_{cc}/\varepsilon_{co})$, **(b)** at failure $(\varepsilon_{cr}/\varepsilon_{or})$.

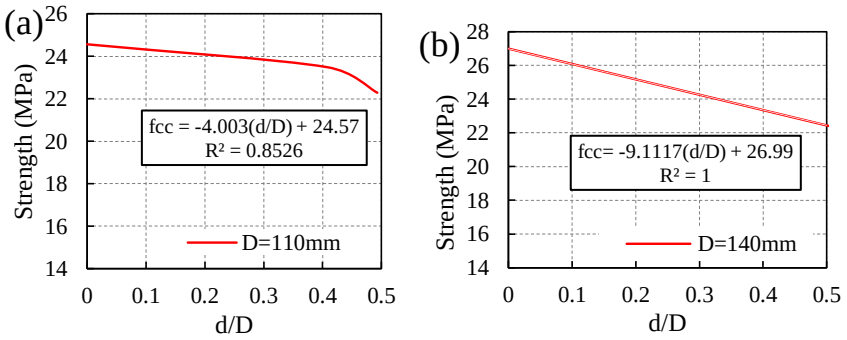

Fig. (11). Effect of hollow ratio on the strength.

Table 7. The effect of a hollow ration on the strength of double skin concrete-filled uPVC tube specimens.

	Internal Tube				Ext. Tube						
Label	t_1	D_1	***d***	***t***	***D***	***h***	***h/D***	***D/h***	**(D-d)/D**	**Strength (MPa)**	
C3P3H1	0	0	0		3	110	220	2	0	1	26.99
C3P4H1	0	0	0		3	140	280	2	0	1	24.57
C3P3H2	0	0	0		3	110	440	4	0	1	24.59
C3P3H3	0	0	0		3	110	660	6	0	1	23.15
C3P3H4	0	0	0		3	110	880	8	0	1	20.98
C3D1H1	3	63	57		3	110	220	2	0.52	0.48	22.27
C3D2H1	3	75	69		3	140	280	2	0.49	0.51	22.29
C3D3H1	3	63	57		3	140	280	2	0.41	0.59	23.49
C3D1H2	3	63	57		3	110	440	4	0.52	0.48	20.14

(Table 7) contd.....

	Internal Tube				Ext. Tube						
Label	t_1	D_1	*d*	*t*	*D*	*h*	*h/D*	*D/h*	**(D-d)/D**	**Strength (MPa)**	
C3D1H3	3	63	57		3	110	660	6	0.52	0.48	18.37
C3D3H2	3	63	57		3	140	560	4	0.41	0.59	20.71
C3D3H3	3	63	57		3	140	840	6	0.41	0.59	18.43

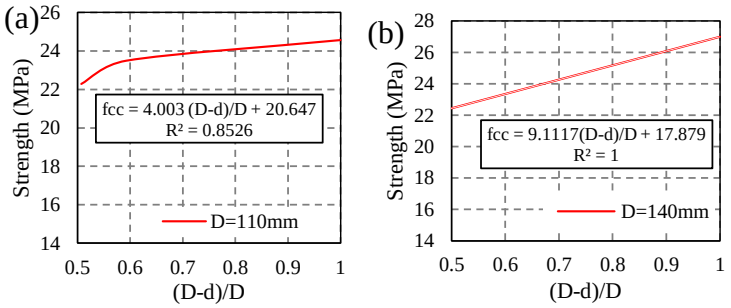

Fig. (12). Effect of overall thickness on the strength.

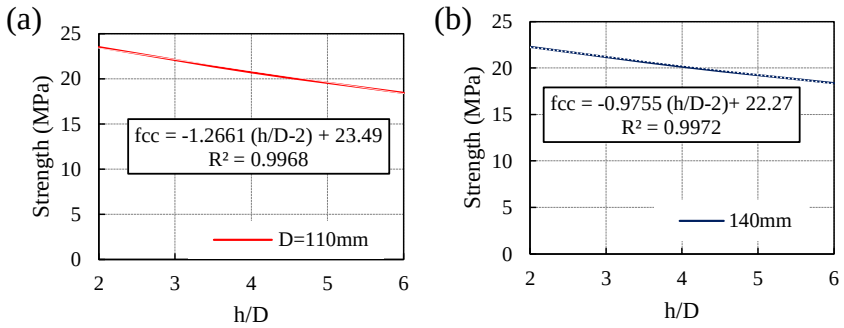

Fig. (13). Effect of aspect ratio (h/D) on strength.

Woldemariam *et al*. [2] have developed an analytical expression for concrete-filled single skin uPVC tube equivalent cylinders that relates the concrete strength, tensile strength, diameter, and thickness of the confining material as shown in Eq. (1):

$$f_{cc} = f_{co} + \frac{2.7 f_l}{(f_{co})^{0.394}(2t/D)^{0.453}} \quad \textbf{(1)}$$

An expression for double skin concrete-filled uPVC tube equivalent cylinder was developed based on Figs. (**11** and **12**) and Eq. 1. The results on two different 2t/D and three d/D ratios are used to define the relation in Eq. 2 and 3.

$$f_{cc(P4)} = -4.003\left(\frac{d}{D}\right) + 24.57 \quad \textbf{(2)}$$

$$f_{cc(P3)} = -9.1117\left(\frac{d}{D}\right) + 26.99 \quad \textbf{(3)}$$

From the above two equations (Eq. 2 and 3), the two constants are equal to the peak strength of (p=90 &110mm) concrete filled single skin uPVC tubular specimens with h/D =2 and can be calculated by the expression in Eq. 1. The coefficients (coef 1 = -4.0003 & coef 2 = -9.1117) are dependent on 2t/D.

Thus, the strength of double skin concrete-filled uPVC tube specimen can be calculated by the expression in Eq. 4.

$$f_{cc} = f_{co} + \frac{2.7 f_l}{(f_{co})^{0.394}(2t/D)^{0.453}} - 130 * 10^3 \left(\frac{2t}{D}\right)^{3.28} * \left(\frac{d}{D}\right) \quad \textbf{(4)}$$

3.4. Effect of Aspect Ratio

Fig. (**13**) shows the effect of aspect ratio (h/D) on strength. The strength decreased as the aspect ratio increased. An expression to predict the strength of double skin concrete filled uPVC tube specimens for different aspect ratios is developed. As the aspect ratio (h/D) increased from 2 to 6, the peak strength decreased, as shown in Fig. (**13**) and Table **7**. The results of two different 2t/D and three h/D ratios are used to define the relation shown in Eq 5.

$$f_{cc(P4)} = -1.2661\left(\frac{h}{D} - 2\right) + 23.49 \quad \textbf{(5)}$$

$$f_{cc(P3)} = -0.9755\left(\frac{h}{D} - 2\right) + 22.27 \quad \textbf{(6)}$$

From the above equation (Eq. 5 and 6), the two constants are equal to the peak strength of (p=90 &110mm) double skin concrete-filled uPVC tube with h/D =2 in Eq. 4. The coefficients (coef 1= -1.2661 & coef 2= -0.9755) are dependent on 2t/D. Hence, $coef = -0.05\left(\frac{2t}{D}\right)^{-1.04}$.

The general equation in Eq 7. was developed by combining Eq. 4, Eq. 5, and Eq. 6.

$$f_{cc} = f_{co} + \frac{2.7f_l}{(f_{co})^{0.394}(2t/D)^{0.453}} - 130 * 10^3\left(\frac{2t}{D}\right)^{3.28} * \left(\frac{d}{D}\right) - 0.05\left(\frac{2t}{D}\right)^{-1.04}\left(\frac{h}{D} - 2\right) \quad \textbf{(7)}$$

The model in Eq. 7 was used to predict the peak strength, compared with the experimental result (Fig. **14**). The accuracy of the model was evaluated by using an Average Absolute Error (AAE), as defined in Eq. 8. The proposed model predicted the peak strength reasonably well with an AAE of 2.13%.

$$MAE = \frac{\sum_{i=1}^{N}\left|\frac{(fcc)_{Model} - (fcc)_{Exp}}{(fcc)_{Exp}}\right|}{N} * 100 \quad \textbf{(8)}$$

3.5. Axial Stress-strain Behavior

Fig. (**15**) shows the stress-strain behavior of unconfined concrete equivalent cylinders. The unconfined specimen has undergone a brittle failure after reaching the peak strength whereas both the single and double skin specimens have undergone a ductile failure without a sudden strength loss. Figs. (**16** and **17**) show the stress-strain curve of single and double skin concrete-filled uPVC tube specimens under axial compression load. The result shows that both single and double skin have exhibited similar behavior. When the h/D ratio was increased from 2 to 6, the specimens exhibited a post-peak displacement softening with a strength loss, as shown in Fig. (**17e, f**).

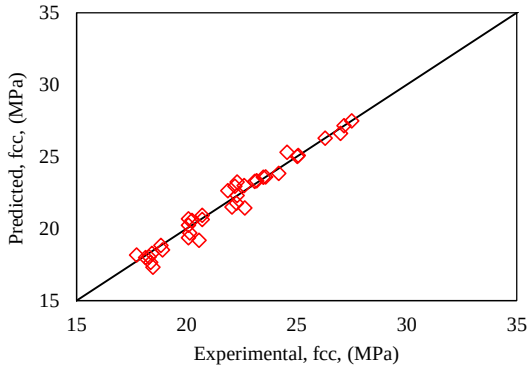

Fig. (14). Performance of the model in predicting the peak strength.

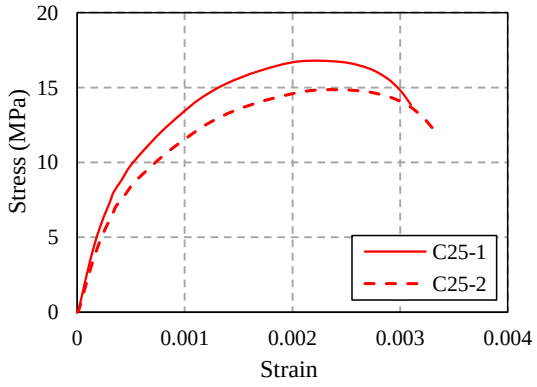

Fig. (15). Stress-Strain curve of the unconfined concrete cylinder of C25.

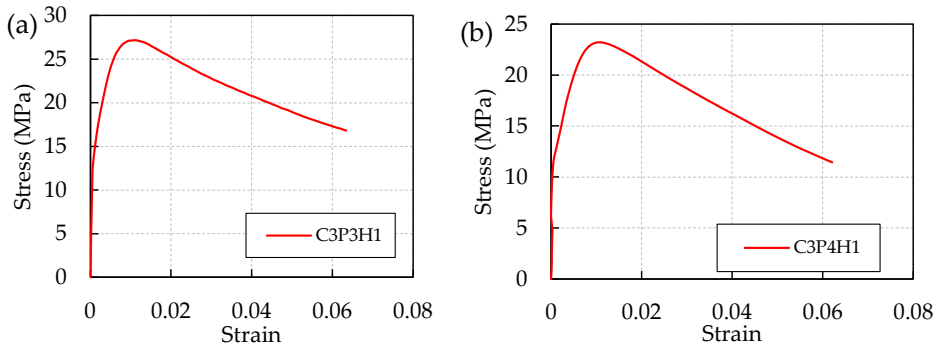

Fig. (16). Stress-strain curve for single skin concrete-filled uPVC specimen with a diameter of **(a)** 110mm, **(b)** 140mm.

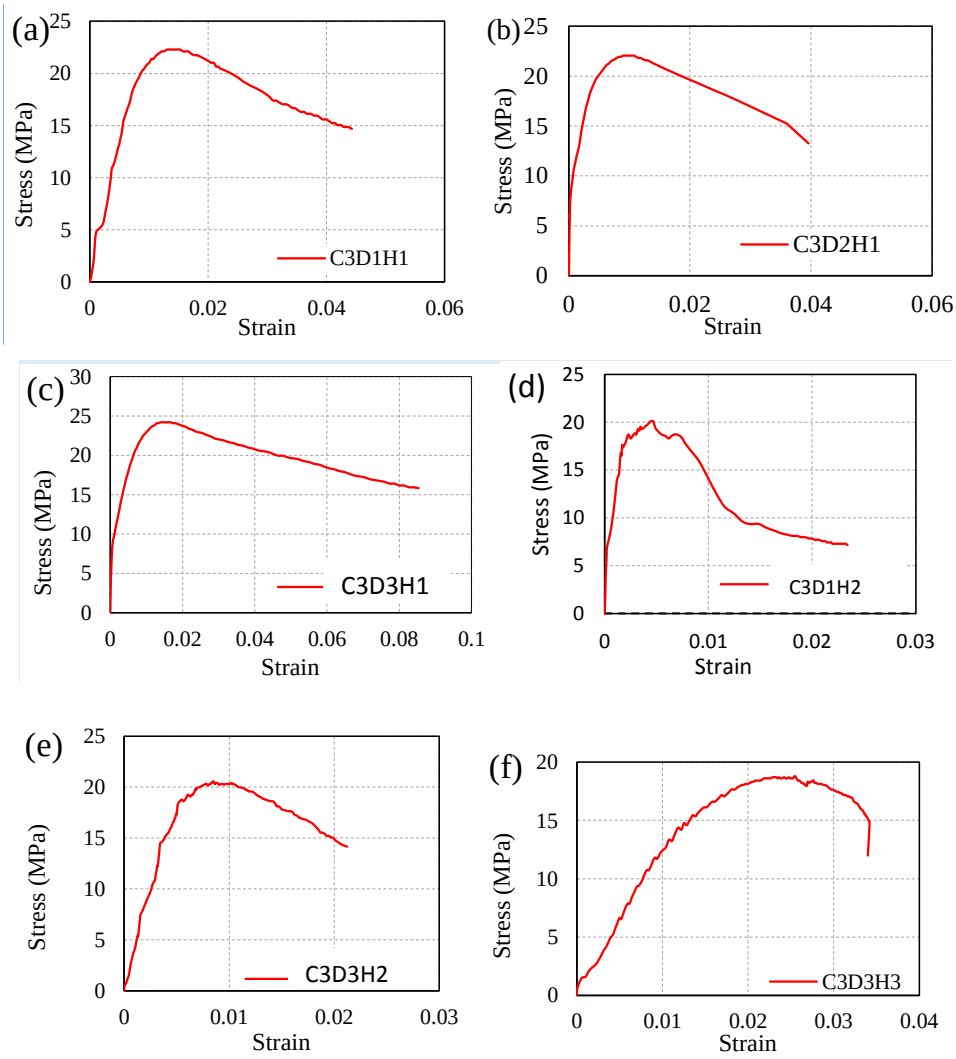

Fig. (17). Stress-strain curve for double skin concrete-filled uPVC specimen.

3.5.1. Ductility and Energy Absorption

Fig. (**18**) shows the parameters used to calculate the ductility factor and energy absorption. The ductility factor is the ratio of strain at fracture strength to strain at maximum elastic strength [36 - 39] and it was calculated by the expression given in Eq. 9. Fig. (**19**) and Table **8** demonstrates the results on the ductility factor of unconfined concrete, single skin and double skin concrete-filled uPVC tube specimens. For single and double skin specimens, the ductility factor increased by 3.7 to 23.45 times compared to the unconfined concrete specimens.

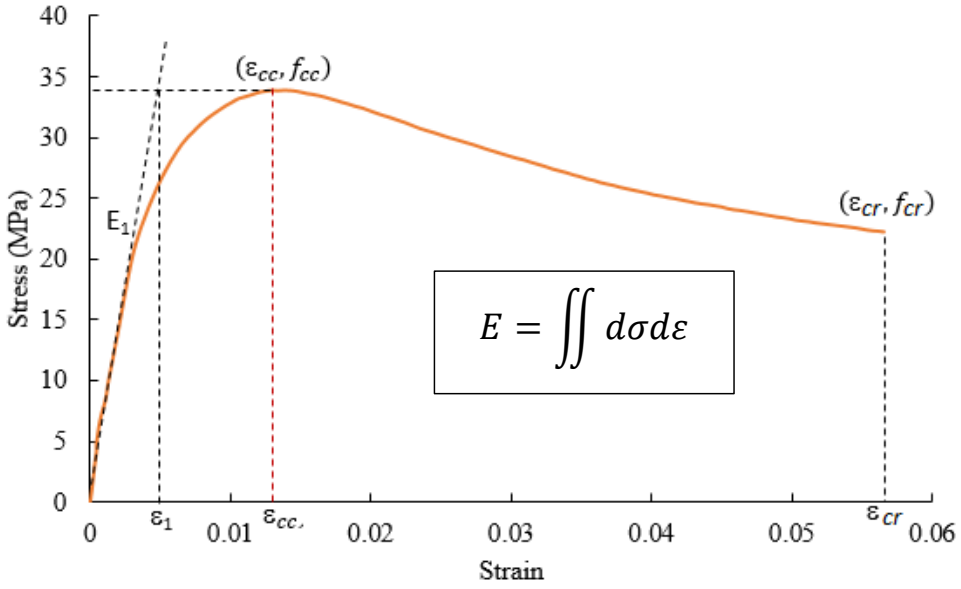

Fig. (18). Stress-strain response parameters used to calculate the ductility factor and energy absorption.

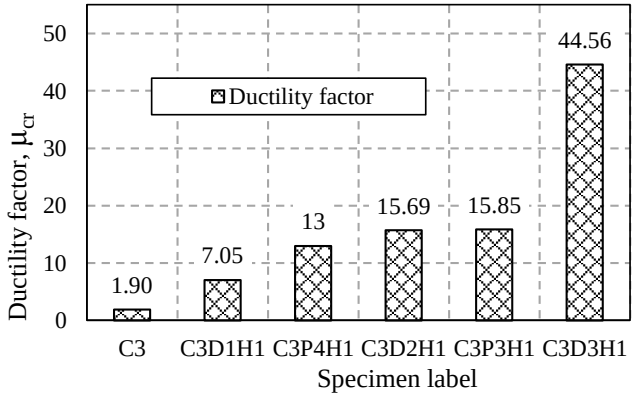

Fig. (19). Ductility factor for unconfined, single and double skin specimens.

Table 8. Average maximum strength, strain, strength enhancement, energy absorption, and ductility Factor.

Label	f_{co}	f_{cc}	ε_{co}	ε_{cc}	ε_1	ε_{cr}	f_{cc}/f_{co}	$\varepsilon_{cc}/\varepsilon_{co}$	μ_{cr}	E
C3	16.89		0.0029		0.0017	0.0033			1.89	0.038
C3P3H1		26.99		0.0098	0.0033	0.0515	1.60	3.43	15.85	1.14
C3P4H1		24.57		0.0094	0.0050	0.0650	1.45	3.32	13.00	1.11
C3P3H2		24.59		0.0331	0.0060	0.10000	1.02	10.18	16.67	1.99
C3P3H3		23.15		0.0175	0.0060	0.06580	0.96	5.40	30.54	1.18
C3P3H4		20.98		0.0187	0.0055	0.08600	0.87	5.76	16.23	1.29
C3D1H1		22.27		0.0130	0.0065	0.0458	1.32	4.56	7.05	0.79
C3D2H1		22.29		0.0090	0.0020	0.0314	1.32	3.16	15.69	0.59
C3D3H1		23.49		0.0130	0.0020	0.0891	1.39	4.56	44.56	1.73
C3D1H2		20.14		0.0045	0.0015	0.0234	1.19	1.56	15.61	0.29
C3D1H3		18.37		0.0124	0.0044	0.0151	1.09	4.35	3.43	0.21
C3D3H2		20.71		0.0084	0.0040	0.0247	1.23	2.95	6.17	0.39
C3D3H3		18.43		0.0255	0.0130	0.0340	1.09	8.94	2.62	0.47

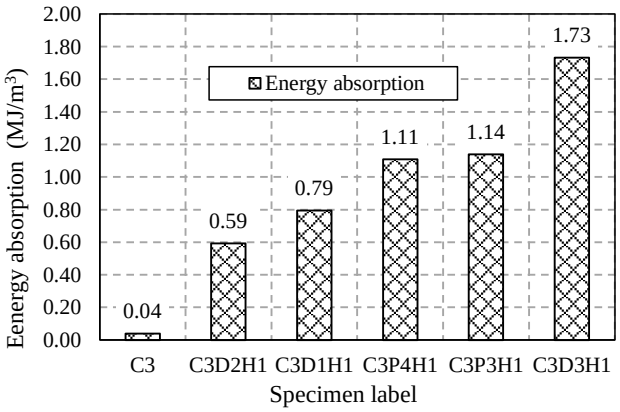

Fig. (20). Energy absorption for unconfined, single and double skin specimens.

The energy absorption is the area under the stress-strain curve [36, 38 - 41] and it was obtained by integrating the stress-strain curve (see Eq.10). Fig. (**20**) and Table **8** shows the results on the energy absorption capacity of unconfined concrete, single and double skin concrete-filled uPVC tube specimens under axial compression loads. The energy absorption capacity of single and double skin specimens increased by 14.75 to 43.25 times compared to the unconfined concrete specimens.

$$\mu_{cf} = \frac{\varepsilon_{cr}}{\varepsilon_1} \quad \textbf{(9)}$$

$$E = \iint d\sigma d\varepsilon \quad \textbf{(10)}$$

CONCLUSION

This paper has presented the results on the behavior of single and double skin concrete-filled uPVC tube specimens subjected to axial compression loads. The following conclusions are drawn based on the results reported in this paper.

- Both single and double skin concrete-filled uPVC tubular specimens exhibited very ductile behavior under axial compression load compared to the unconfined concrete specimens. For concrete-filled single and double skin uPVC tubular specimens, the strength, ductility, and energy absorption increased by more than 1.32, 3.75 and 14.75 times compared to the unconfined concrete specimens, respectively.
- The failure modes observed during the experimental program were the brittle crushing, drum, shear, and buckling type failure modes. The unconfined concrete has undergone a brittle failure. Drum type failure mode is the most prevalent failure modes observed in both single and double skin specimens with lower aspect ratios. For double skin specimen, the specimen expanded outward similar to the single skin creating drum-type failure. The internal tube of double skin specimen has undergone local buckling. Also, buckling type failure mode was observed on both CFSUT and CFDUT specimens with higher aspect ratios.
- As expected, the use of uPVC tube in single and double skin concrete-filled tubular specimens increased the strength. The strength of CFDUT decreased as the hollow ratio (d/D) and aspect ratio (h/D) increased.
- The peak strength and strain enhancement ratios (f_{cc}/f_{co} and $\varepsilon_{cc}/\varepsilon_{co}$) of CFSUT and CFDUT increased by 1.32 and 3.16 times compared to the unconfined respectively.
- The peak strength model predicted the peak strength of axially loaded concrete-filled uPVC tube column with a mean absolute error of 2.13%.

Ductile behavior with improved strength of concrete filled single and double skin uPVC tubular system has been observed during the study. The concrete-uPVC tube hybrid system has the potential to be used for building columns, bridge piers, highway head structures, piles, electric and telecom poles. However, more work is required on uPVC confined concrete columns under eccentric, lateral, cyclic and pure bending load to further understand its performance under different loading conditions.

NOMENCLATURE

E	=	Energy Absorption Capacity
uPVC	=	Unplasticized Polyvinyl Chloride
t	=	Thickness
RC	=	Reinforced Concrete
PVC	=	Polyvinyl Chloride
h	=	height
FRP	=	Fiber-Reinforced Polymer
D	=	Diameter
σ_1, σ_2 **and** σ_3	=	Principal Stresses
μ_{cr}	=	Ductility Factor
f_{co}	=	Unconfined Compressive Strength
f_{cc}	=	Confined Compressive Strength
f_y	=	Yield Stress of uPVC
f_l	=	Lateral Confining Pressure
k_1	=	Confinement Coefficient
ε_{cc}	=	Strain at Max Strength of Confined Concrete

ε_1 = Elastic Strain at Max Strength

E = Energy Absorption Capacity

ε_{cr} = Strain at Failure Load

ε_{co} = Strain at Max Strength of Unconfined Concrete

AUTHOR CONTRIBUTIONS

Author Contributions: Conceptualization, A.M.W., W.O.O. and T.N.; Methodology, A.M.W., W.O.O. and T.N.; Experiment and data collection, A.M.W.; software, A.M.W.; Analysis, A.M.W.; writing-original draft preparation, A.M.W.; writing-review and editing, A.M.W., W.O.O. and T.N.

CONSENT FOR PUBLICATION

Not applicable.

AVAILABILITY OF DATA AND MATERIALS

The data that support the findings of this study are available from the corresponding author upon request.

FUNDING

Material support from the African Union Commission (AUC) and Africa-ai-Japan Project 2018-2019 to carry out the experiment is gratefully acknowledged.

CONFLICT OF INTEREST

The authors declare no conflict of interest, financial or otherwise.

ACKNOWLEDGMENTS

The authors sincerely thank the African Union Commission (AUC) and Africa-ai-Japan Project for funding this research.

REFERENCES

[1] P. Sarir, J. Chen, P.G. Asteris, D.J. Armaghani, and M.M. Tahir, "Developing GEP tree-based, neuro-swarm, and whale optimization models for evaluation of bearing capacity of concrete-filled steel tube columns", *Eng. Comput.,* pp. 1-19, 2019.

[2] A. M. Woldemariam, W. O. Oyawa, and T. Nyomboi, "Structural Performance of uPVC Confined Concrete Equivalent Cylinders Under Axial Compression Loads", *Buildings,* vol. 9, no. 4, p. 83, 2019. [http://dx.doi.org/10.3390/buildings9040082]

[3] K.N. Gathimba, W.O. Oyawa, and G.N. Mang'uriu, Performance of UPVC Pipe Confined Concrete Columns in Compression. MSc. Thesis*,* 2015.

[4] W.O. Oyawa, N.K. Gathimba, and G.N. Mang'uriu, "Structural response of composite concrete filled plastic tubes in compression", *Steel Compos. Struct.,* vol. 21, no. 3, pp. 589-604, 2016. [http://dx.doi.org/10.12989/scs.2016.21.3.589]

[5] J. Xue, H. Li, L. Zhai, X. Ke, W. Zheng, and B. Men, "'"Analysis of mechanical behavior and influencing factors of high strength concrete columns with PVC pipe under repeated loading," Xi'An Jianzhu Keji Daxue Xuebao/Journal Xi'An Univ", *Archit. Technol.,* vol. 48, pp. 24-28, 2016.

[6] K. Wang, and B. Young, *Fire resistance of concrete-filled high strength steel tubular columns.,* vol. 71. Thin-Walled Struct, 2013, pp. 46-56.

[7] N. Jamaluddin, "Experimental Investigation of Concrete Filled PVC Tube Columns Confined By Plain PVC Socket", *MATEC Web Conf.,* vol. vol. 103, 2017 [http://dx.doi.org/10.1051/matecconf/201710302006]

[8] M. Fakharifar, and G. Chen, "Compressive behavior of FRP-confined concrete-filled PVC tubular columns", *Compos. Struct.,* vol. 141, pp. 91-109, 2016. [http://dx.doi.org/10.1016/j.compstruct.2016.01.004]

[9] M. Fakharifar, and G. Chen, "FRP-confined concrete filled PVC tubes : A new design concept for ductile column construction in seismic regions", *Constr. Build. Mater.,* vol. 130, pp. 1-10, 2017. [http://dx.doi.org/10.1016/j.conbuildmat.2016.11.056]

[10] P.K. Gupta, and V.K. Verma, "Study of concrete-filled unplasticized poly-vinyl chloride tubes in marine environment", *Proc. Inst. Mech. Eng. Part M. J. Eng. Marit. Environ.,* vol. 230, no. 2, pp. 229-240, 2014.

[11] A.S. Saadoon, *Experimental and Theoretical Investigation of PVC-Concrete Composite Columns.,* University of Basrah, 2010.

[12] C.E. Kurt, "Concrete Filled Structural Plastic Columns", *J. Struct. Div.,* vol. 104, no. 1, pp. 55-63, 1978.

[13] N.A. Abdulla, "Influence of plastic pour-in form on mechanical behavior of concrete", *Structures,* vol. 19, pp. 193-202, 2019. [http://dx.doi.org/10.1016/j.istruc.2019.01.007]

[14] M. Marzoucka, and K. Sennah, "Concrete filled PVC tubes as compression members", *International seminar, Composite material in concrete construction,* 2002 pp. 31-38

[15] J.Y. Wang, and Q.B. Yang, "Investigation on compressive behaviors of thermoplastic pipe confined concrete", *Constr. Build. Mater,* vol. 35, pp. 578-585, 2012. [http://dx.doi.org/10.1016/j.conbuildmat.2012.04.017]

[16] P.K. Gupta, "Confinement of concrete columns with unplasticized Poly-vinyl chloride tubes", *Int. J. Adv. Struct. Eng.,* vol. 5, no. 1, pp. 1-8, 2013. [http://dx.doi.org/10.1186/2008-6695-5-19]

[17] F. Zhou, and W. Xu, "Cyclic loading tests on concrete-filled double-skin (SHS outer and CHS inner) stainless steel tubular beam-columns", *Eng. Struct.,* vol. 127, pp. 304-318, 2016. [http://dx.doi.org/10.1016/j.engstruct.2016.09.003]

[18] R. Imani, G. Mosqueda, and M. Bruneau, "Finite element simulation of concrete-filled double-skin tube columns subjected to post-earthquake fires", *J. Struct. Eng.,* vol. 141, no. 12, 2015. 04015055. [http://dx.doi.org/10.1061/(ASCE)ST.1943-541X.0001301]

[19] H. Huang, L. Han, Z. Tao, and X. Zhao, "Analytical behaviour of concrete-filled double skin steel tubular (CFDST) stub columns", *J. Construct. Steel Res.,* vol. 66, no. 4, pp. 542-555, 2010. [http://dx.doi.org/10.1016/j.jcsr.2009.09.014]

[20] W. Li, L.H. Han, and T.M. Chan, "Tensile behaviour of concrete-filled double-skin steel tubular members", *J. Construct. Steel Res.,* vol. 99, pp. 35-46, 2014. [http://dx.doi.org/10.1016/j.jcsr.2014.03.011]

[21] S. Aghdamy, D.P. Thambiratnam, M. Dhanasekar, and S. Saiedi, "Effects of load-related parameters on the response of concrete-filled double-skin steel tube columns subjected to lateral impact", *J. Construct. Steel Res.,* vol. 138, pp. 642-662, 2017. [http://dx.doi.org/10.1016/j.jcsr.2017.08.015]

[22] M.F. Hassanein, O.F. Kharoob, and Q.Q. Liang, "Circular concrete-filled double skin tubular short columns with external stainless steel tubes under axial compression", *Thin-walled Struct.,* vol. 73, pp. 252-263, 2013. [http://dx.doi.org/10.1016/j.tws.2013.08.017]

[23] European Standard, *EN 197-130 Cement. Composition, specifications and conformity criteria for common cements.,* European Standard: Brussels, Belgium, 2011.

[24] British Standard Institution, *BS EN 932-1 Tests for General Properties of Aggregates: Part 1. Methods for Sampling.,* British Standard Institution: London, 1997.

[25] British Standard Institution, *BS EN 933-1Tests for Geometrical Properties of Aggregates Part 1 : Determination of Particle Size Distribution— Sieving Method.,* British Standard Institution: London, UK, 2012.

[26] British Standard Institution, *BS EN 933-2 Tests for geometrical properties of aggregates. Determination of particle size distribution. Test sieves, nominal size of apertures.,* BSI Standards Ltd.: London, UK, 1996.

[27] ASTM International, *ASTM D638 Standard test method for tensile properties of plastics.,* ASTM: West Conshohocken, PA, USA, 2014.

[28] British Standard Institution, *BS EN 1097-6 Tests for Mechanical and Physical Properties of Aggregates Part 6 : Determination of Particle Density and Water Absorption.,* BSI Standards Ltd.: Brussels, Belgium, 2013.

[29] British Standard Institution, *BS EN 1097-5 Tests for mechanical and physical properties of aggregates Part 5. Determination of the water content by drying in a ventilated oven.,* London, UK: British Standards

Institution (BSI), 2008.

[30] British Standard Institution, *BS EN 206:2013 Concrete. Specification, performance, production and conformity.,* 2013.

[31] British Standard Institution, *BS 8500-1:2006+A1:2012 Concrete. Complementary British Standard to BS EN 206-1. Method of specifying and guidance for the specifier.,* London, UK, 2012.

[32] British Standard Institution, *BS EN 12350-1 Testing fresh concrete, Part 1: Sampling Fresh Concrete.,* BSI Standards Ltd.: London, UK, 2009.

[33] British Standard Institution, *BS EN 12350-2 Testing Fresh Concrete, Part 2: Slump Test.,* BSI Standards Ltd.: London, UK, 2009.

[34] British Standard Institution, *BS EN 12350-6 Testing Fresh Concrete, Part 6: Fresh Density.,* BSI Standards Ltd.: London, UK, 2009.

[35] British Standard Institution, *BS 1881-103 Testing Concrete, Part 103: Method for Determination of Compacting Factor.,* BSI Standards Ltd.: London, UK, 1993.

[36] C. Cui, and S.A. Sheikh, "Experimental Study of Normal- and High-Strength Concrete Confined with Fiber-Reinforced Polymers", *J. Compos. Constr.,* vol. 14, no. 5, pp. 553-561, 2010. [http://dx.doi.org/10.1061/(ASCE)CC.1943-5614.0000116]

[37] D. Najdanović, and B. Milosavljević, "Strength and ductility of concrete confined circular columns", *J. Croat. Assoc. Civ. Eng.,* vol. 66, pp. 417-423, 2014.

[38] X-H. Zhang, X-B. Lu, L-M. Zhang, S-Y. Wang, and Q-P. Li, "Experimental study on mechanical properties of methane-hydrate-bearing sediments", *Lixue Xuebao,* vol. 28, no. 5, pp. 1356-1366, 2012. [http://dx.doi.org/10.1007/s10409-012-0142-3]

[39] Y.F. Wu, "The effect of longitudinal reinforcement on the cyclic shear behavior of glass fiber reinforced gypsum wall panels: tests", *Eng. Struct.,* vol. 26, no. 11, pp. 1633-1646, 2004. [http://dx.doi.org/10.1016/j.engstruct.2004.06.009]

[40] J. Wang, "Investigation on compressive behaviors of thermoplastic pipe confined concrete", *Constr. Build. Mater.,* vol. 35, pp. 578-585, 2014.

[41] A.I. Karabinis, and T.C. Rousakis, "Concrete confined by FRP material: A plasticity approach", *Eng. Struct.,* vol. 24, no. 7, pp. 923-932, 2002. [http://dx.doi.org/10.1016/S0141-0296(02)00011-1]